buildings

MDPI

Article

Mechanical Properties of Limestone Under Different Confining Pressures and Wet–Dry Cycles

Zongli Yang [1], Shaowu Zhou [1], Peng Lin [2], Ruinan An [2], Guoyong Duan [3,*] and Zhongyan Zhao [3]

[1] China Three Gorges Construction (Group) Co., Ltd., Chengdu 610041, China; yang_zongli@ctg.com.cn (Z.Y.); zhou_shaowu@ctg.com.cn (S.Z.)
[2] Department of Hydraulic Engineering, Tsinghua University, Beijing 100084, China; celinpe@tsinghua.edu.cn (P.L.); arn20@mail.tsinghua.edu.cn (R.A.)
[3] College of Electrical Engineering and New Energy, China Three Gorges University, Yichang 443002, China; zhaozhongyan@ctgu.edu.cn
* Correspondence: duanguoyong@ctgu.edu.cn; Tel.: +86-17337328167

Abstract

During the operation of large reservoirs, slope rock masses at different elevations are subjected to confining pressure variation and alternating wet–dry cycles induced by water-level fluctuations, resulting in the evolution of their mechanical properties. To investigate this issue, conventional triaxial compression tests were conducted on limestone from Badong County in the Three Gorges Reservoir area under confining pressures of 5–20 MPa and 0–50 wet–dry cycles. The results show that confining pressure significantly enhances limestone strength, whereas wet–dry cycles induce a progressive deterioration in mechanical properties. Under the same confining pressure, the deterioration exhibits a staged characteristic, with a rapid decrease at the early stage followed by a slower decline. Higher confining pressure effectively suppresses crack propagation and mitigates the degradation caused by wet–dry cycling. Meanwhile, wet–dry cycles promote the transition of the failure mode from single-fracture failure to multi-fracture fragmentation. The elastic modulus, cohesion, and internal friction angle all decrease exponentially with increasing wet–dry cycles. Based on damage mechanics theory, a constitutive relationship considering wet–dry cycle effects was established to characterize rock stiffness degradation and its influence on the overall mechanical response. The proposed model effectively describes the evolution of mechanical parameters and deformation characteristics under wet–dry cycling conditions. This study provides an experimental and theoretical basis for evaluating the long-term stability of reservoir slopes.

Keywords: wet–dry cycle; confining pressure effect; mechanical properties; mutual influence

Check for updates

Academic Editor: Oldrich Sucharda

Received: 10 May 2026
Revised: 9 July 2026
Accepted: 31 July 2026
Published: 2 August 2026

Copyright: © 2026 by the authors. Licensee MDPI, Basel, Switzerland. This article is an open access article distributed under the terms and conditions of the Creative Commons Attribution (CC BY) license.

1. Introduction

As a typical carbonate rock, limestone is widely distributed in engineering rock masses such as reservoir banks, slopes, tunnels, and mines. In these environments, the rock mass is often subjected simultaneously to the confining pressure provided by in situ stress and periodic wet–dry cycles induced by groundwater fluctuations or climatic precipitation [1,2]. Particularly in large reservoir areas, the rock mass within the water-level fluctuation zone undergoes repeated drying–wetting alternations due to periodic water-level changes, while also bearing confining pressures that vary with depth [3,4]. This long-term coupled effect of "stress–seepage–chemistry" multi-field interaction leads to mineral dissolution, microcrack initiation, and propagation within the rock mass, resulting in the progressive deterioration

of its physical and mechanical properties, which poses a serious threat to the long-term stability of engineering structures [5,6].

The deterioration effect of wet–dry cycles on rock mechanical properties has been extensively documented. It is widely recognized that cyclic water–rock interaction accelerates internal damage through mechanisms such as pore pressure change, soluble salt crystallization/dissolution, and physicochemical weakening of grain boundaries, leading to significant reductions in strength, elastic modulus, and other key parameters [7–9]. The degradation often follows a nonlinear trend, characterized by rapid initial deterioration that gradually stabilizes [10,11]. Recent studies have further diversified, examining various rock types and specific degradation processes under wet–dry conditions. For instance, the deterioration of jointed sandstone [12], argillaceous siltstone [13], cement-stabilized loess [14], and red-bed mudstone [15] has been investigated. Research has also extended to related cyclic processes like freeze–thaw cycles and their impact on wave velocity and mechanical indices in limestone [16,17], as well as the creep behavior of carbonaceous shale under dry–wet cycles [18].

Concurrently, significant research efforts have focused on the mechanical response and constitutive modeling of rocks under triaxial stress states. The strengthening effect of confining pressure in suppressing crack propagation and enhancing rock ductility and peak strength is well established [19,20]. Studies range from miniature triaxial tests for parameter estimation [21] and large-scale triaxial tests on weathered rockfill considering particle breakage [22], to investigations of time-dependent behavior and permeability evolution under hydro-mechanical coupling [23] and triaxial creep characteristics in high-stress environments [24]. The development of advanced constitutive models, including multiscale models for freeze–thaw rocks under compression [25] and damage evolution models for karst-affected rock [26], reflects the growing sophistication in characterizing rock behavior.

A prominent and evolving research frontier involves the coupled effects of multiple factors. Studies increasingly consider the interplay between environmental cycles and mechanical loading. Examples include research on fracture process zone development under combined wet–dry cycles and temperature dynamic tensile behavior and energy evolution under dry–wet cycles [27], and the mechanical properties of limestone under cyclic loading with varying moisture content [28]. Furthermore, the role of specific chemical environments is being scrutinized, such as degradation under alkaline wet–dry cycles, dynamic dissolution by CO_2 solution [29], and the influence of acidic cycles on sandstone [30]. The integration of advanced monitoring techniques, like acoustic emission to study fracture behavior under coupled pressures and cycles [31], is also enhancing the understanding of degradation mechanisms.

Despite these advances, a discernible research gap persists. Many studies on wet–dry cycles are conducted under uniaxial or low-confining-pressure conditions, which do not fully represent the true triaxial stress state of in situ engineering rock masses. Conversely, studies focusing on confining pressure effects often neglect the time-dependent property deterioration caused by long-term environmental hydration–dehydration processes. Although the coupling effect is recognized, systematic investigation into how different levels of confining pressure (particularly within the practically relevant medium-to-low range of 5–20 MPa for reservoir slopes) modulate the damage rate, degradation pathway, and ultimate failure mode induced by repeated wet–dry cycles remains insufficient. The quantitative evolution laws of mechanical parameters and the underlying micromechanical mechanisms under this specific coupled condition are not yet fully elucidated.

To fill the gaps in related research, in this paper, we take typical limestone slopes in Badong County, Three Gorges Reservoir area, as the research object. A series of conventional

triaxial compression tests was conducted under coupled conditions of confining pressures of 5, 10, 15, and 20 MPa and 0, 5, 10, 15, 25, and 50 wet–dry cycles. The research focuses on ① analyzing the evolution characteristics of intact stress–strain curves of the limestone; ② quantitatively revealing the deterioration laws of key mechanical parameters such as peak strength, elastic modulus, cohesion, and internal friction angle; ③ elucidating the inhibitory effect of confining pressure on wet–dry cycle damage; and ④ exploring the changing characteristics of failure modes with cyclic action. The research results can provide an important experimental basis and theoretical support for the long-term stability evaluation and engineering protection measures of rock slopes in reservoir water-level fluctuation zones under water–mechanical coupling.

2. Test Overview

2.1. Sample Preparation

Badong County in the Three Gorges Reservoir area is located in a typical karst landform region with widespread limestone distribution. Therefore, the limestone near the site of the embedded pile foundation of the local power transmission line was selected as the research object of the surrounding rock mass. The original rock was processed into standard cylindrical specimens with a diameter of 50 mm and a height of 100 mm (height-to-diameter ratio of 2:1). The end faces were ground smooth to ensure that the flatness and parallelism met the test requirements, as shown in Figure 1. The figure shows some of the limestone specimens used in this study. The Badong limestone used in the test mainly contains mineral components common in karst areas, such as calcite, quartz, and iron oxides, with calcite as the main component, a small amount of quartz, and almost no clay minerals.

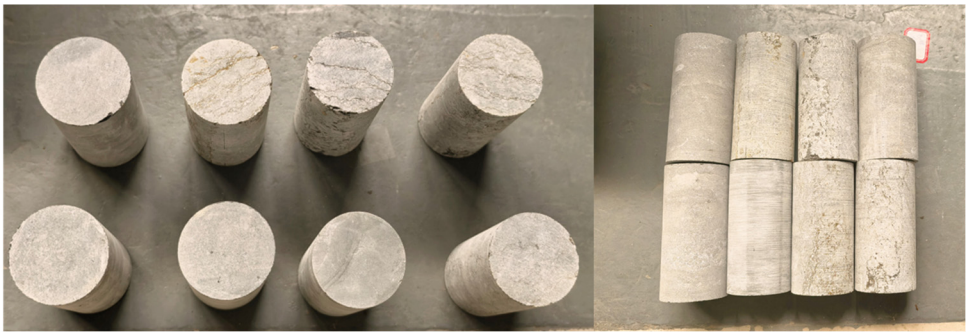


Figure 1. Standard limestone samples.

To reduce the impact of sample dispersion on the test results, samples with relatively concentrated and stable distributions of longitudinal wave velocity and porosity values were prioritized, provided the samples were undamaged, thus ensuring the uniformity of their physical properties and the reliability of the research results.

To investigate the influence of wet–dry cycling on limestone deterioration in the Three Gorges Reservoir area, a 10% Na_2SO_4 solution was adopted as the cycling medium [32–34]. Prior to the soaking stage, the limestone specimens were vacuum-saturated to ensure sufficient water penetration. Each wet–dry cycle lasted 3 days and consisted of two stages: immersion in a 10% Na_2SO_4 solution for 48 h and drying in an oven at 80 °C for 24 h. To maintain a constant solution concentration, the Na_2SO_4 solution was periodically renewed throughout the tests. The number of wet–dry cycles was set to 0, 5, 10, 15, 25, and 50.

Although natural reservoir water contains various dissolved ions, the 10% Na_2SO_4 solution was selected as an accelerated deterioration medium to reproduce sulfate-induced water–rock interactions within a practical laboratory timescale. This approach has been

widely adopted in previous studies of limestone degradation under wet–dry cycling conditions and provides a repeatable method for evaluating the evolution of mechanical properties.

2.2. Experimental Equipment

As shown in Figure 2, a triaxial rheometer is an advanced testing device used to study the mechanical behavior and long-term deformation characteristics of soil and rock materials under high-temperature and high-pressure conditions. This instrument can apply independently controlled axial stress and confining pressure to the sample, and can adjust environmental factors such as temperature and pore pressure to simulate the actual stress state underground. By conducting conventional triaxial compression tests and creep tests (such as constant load and graded loading creep), the strength parameters of the material and its deformation characteristics over time can be obtained, thus providing reliable experimental evidence for analyzing the stability of rock masses under complex stress environments and long-term action.



Figure 2. TOPINDUSTRIE triaxial rheometer.

2.3. Test Plan

To systematically study the impact of wet–dry cycles on the mechanical properties of limestone slopes, the typical subtropical monsoon climate, spatial and temporal rainfall distribution, and groundwater chemical environment (high SO_4^{2-} and Na^+ content) of Badong County in the Three Gorges Reservoir area were considered. Taking into account the actual conditions of the reservoir slope rock mass being submerged in water during the rainy season and naturally drying during the non-rainy season, wet–dry cycle conditions were established, and corresponding experimental studies were conducted.

In the experiments, the processed standard limestone samples were divided into 6 groups of 12 specimens each. These samples underwent 0, 5, 10, 15, 25, and 50 wet–dry cycles, respectively, with 0 cycles serving as a control group. After each cycle, the samples were uniformly dried before undergoing conventional triaxial compression tests. The confining pressures were set at 5 MPa, 10 MPa, 15 MPa, and 20 MPa, respectively. The experiment was conducted using a Top Industrie triaxial rheometer (see Figure 1). First, a confining pressure was applied at a rate of 0.05 MPa/s to the target value and held steady. Then, an axial load was applied at a rate of 0.5 MPa/s until the specimen failed. During the experiment, the stress–strain curves, peak intensity, and failure mode were recorded. The specific loading method is shown in Figure 3.

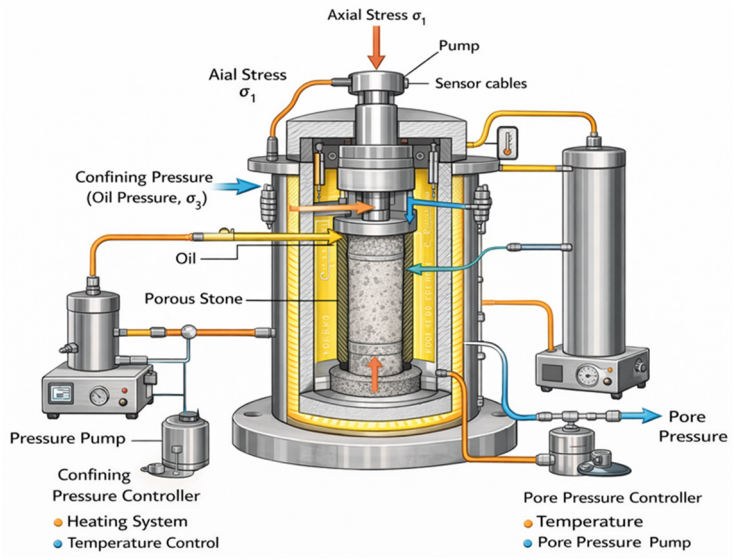


Figure 3. Schematic diagram of the experimental loading scheme.

A conventional triaxial compression loading method was employed in this experiment. The specimen was placed in a pressure chamber, and a uniform confining pressure (σ_3) was applied around the specimen using pressurized oil, while an axial stress (σ_1) was simultaneously applied along the axial direction by a loading piston. The confining pressure and axial stress were controlled by independent systems. During loading, the confining pressure was first increased to a set value at a certain rate and remained stable. Subsequently, an axial load was applied under constant confining pressure until the specimen failed. By recording the stress–strain response and failure characteristics of the specimen during loading, the mechanical parameters and deformation patterns of limestone under different wet–dry cycle numbers and confining pressure conditions were obtained.

Through comparative analysis of the experimental results under different combinations of confining pressure and wet–dry cycle numbers, the evolution law of limestone strength parameters and deformation characteristics was revealed, thus elucidating the mechanical degradation mechanism under wet–dry cycle action and providing an experimental basis for the long-term stability evaluation of reservoir slope rock masses.

3. Results

3.1. Stress–Strain Curve Characteristic Analysis

Figure 4 shows the stress–strain curves of the limestone samples after conventional triaxial compression tests following 0, 5, 10, 15, 25, and 50 cycles of wet and dry compression.

As can be seen from Figure 4, the stress–strain curves of the limestone samples have a generally consistent shape and can be divided into four stages: (1) Initial compaction stage. The curve is concave upwards. In this stage, the original pores and microcracks inside the limestone close under pressure. Under a confining pressure of 5 MPa, the strain in this stage accounts for 18.2% of the total strain. Under a confining pressure of 20 MPa, due to stronger initial constraints, the proportion of compaction strain decreases to 10.5%. (2) Elastic deformation stage. The curve shows linear growth, with the slope being the elastic modulus. The higher the confining pressure, the longer the linear segment. Under a confining pressure of 20 MPa, the stress range in the elastic stage is 92.3% higher than that under 5 MPa, reflecting the strengthening effect of confining pressure on elastic deformation capacity.

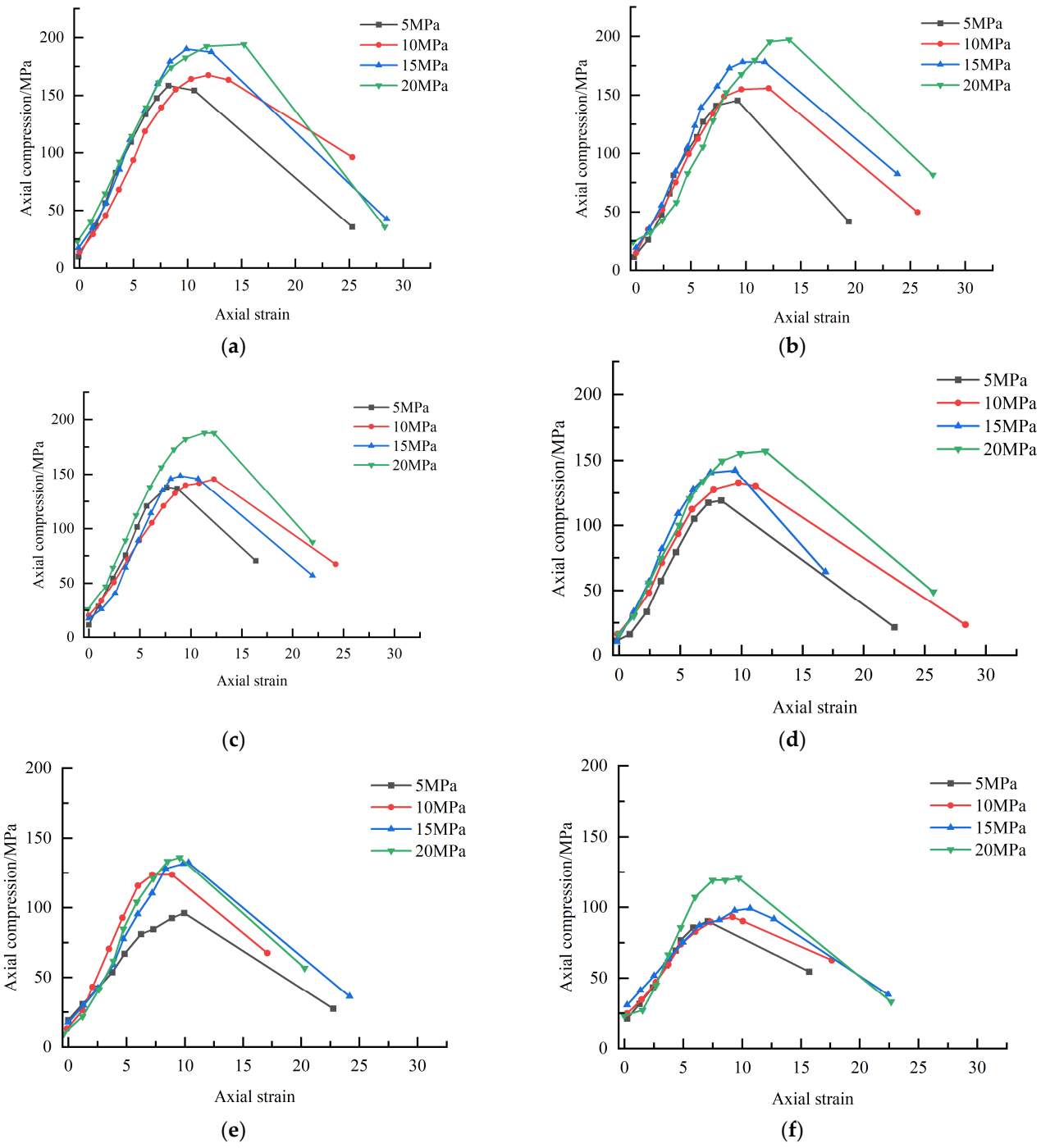


Figure 4. Stress–strain curves of the limestone sample. (**a**) The number of wet–dry cycles is 0. (**b**) The number of wet and dry cycles is 5. (**c**) The number of wet and dry cycles is 10. (**d**) The number of wet and dry cycles is 15. (**e**) The number of wet and dry cycles is 25. (**f**) The number of wet and dry cycles is 50.

(3) Stable crack propagation stage. After the stress exceeds the crack initiation threshold, new microcracks initiate and propagate stably. The crack density gradually increases, and the stress–strain curve deviates from linearity. With increasing confining pressure, the stable crack propagation stage becomes more pronounced, indicating that confining pressure suppresses crack growth and enhances the deformation capacity of the limestone.

(4) Unstable crack propagation and failure stage. As the stress approaches the peak strength, crack propagation becomes unstable and rapidly develops into macroscopic failure surfaces. After the peak stress is reached, the specimen enters the post-peak failure

stage. Under low confining pressure (5 MPa), a pronounced brittle stress drop is observed, whereas under high confining pressure (20 MPa), the post-peak response becomes more gradual and exhibits significant residual strength, indicating enhanced resistance to catastrophic failure.

3.2. Analysis of Damage Characteristics

Figure 5 shows the failure characteristics of some specimens when the confining pressure is 20 MPa.

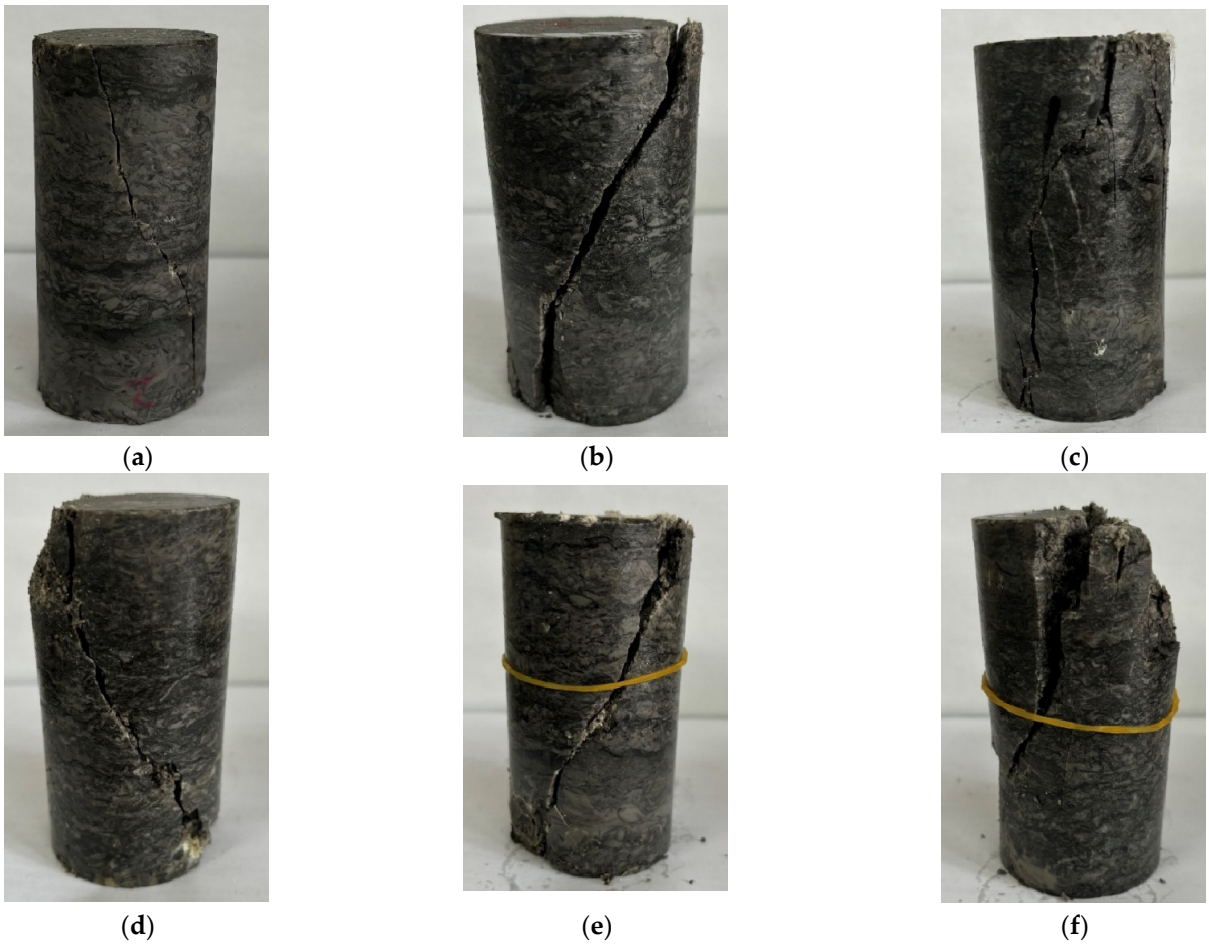


Figure 5. Failure characteristics of some specimens under a confining pressure of 20 MPa. (**a**) The number of wet–dry cycles is 0. (**b**) The number of wet and dry cycles is 5. (**c**) The number of wet and dry cycles is 10. (**d**) The number of wet–dry cycles is 15. (**e**) The number of wet and dry cycles is 25. (**f**) The number of wet and dry cycles is 50.

Analysis of the failure characteristics in Figure 5 shows that in the initial stage (0–5 cycles), the rock sample failure is mainly characterized by a single main crack with relatively regular crack morphology (e.g., only one through-crack appears after 0 cycles, and the main crack expands after 5 cycles, but the overall integrity remains relatively good). The failure mode is mainly "tensile–shear composite failure," characterized by microcrack initiation.

In the development stage (10–15 cycles), the width of the main crack increases significantly, accompanied by the initiation of secondary cracks (e.g., multiple branch cracks appear after 10 cycles, and local spalling occurs in the rock sample after 15 cycles). The failure mode gradually shifts to "multi-crack through-crack failure," and the integrity of

the rock sample begins to decline significantly. This is the result of the combined effects of swelling and shrinkage damage caused by wet–dry cycles and chemical degradation.

Intensification Stage (25–50 cycles): The rock sample failure characteristics exhibit a "fragmentation" trend, with a fully developed crack network (e.g., after 25 cycles, the rock sample needs to be bound to maintain its shape; after 50 cycles, the degree of fragmentation further increases). The failure mode shifts to "brittle splitting failure." At this point, the internal cementation of the rock sample has been significantly weakened, and the cumulative damage from the wet–dry cycles causes a sharp decline in the overall load-bearing capacity of the rock sample, making it more prone to fragmentation upon failure.

4. Discussion

4.1. Analysis of the Influence of Confining Pressure on the Mechanical Properties of Limestone

Figure 6 shows the variation in peak strength values at the time of limestone failure under different wet–dry cycles and different confining pressures.

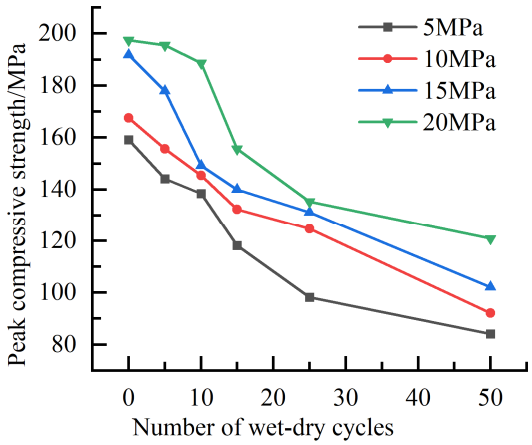


Figure 6. Peak strength variation during limestone failure.

As shown in Figure 6, after 50 wet–dry cycles, the peak compressive strength of the sample decreased by 47.13% at a confining pressure of 5 MPa, 44.67% at 10 MPa, 46.67% at 15 MPa, and 38.75% at 20 MPa. This indicates that the peak compressive strength of the limestone significantly decreased under the same confining pressure with increasing wet–dry cycle count, and the decreasing trend was not linear. The damage and degradation effect of wet–dry cycles on the strength of limestone is non-uniform and cannot be ignored.

Under the same number of wet–dry cycles, the peak strength of the sample showed a significant increasing trend as the confining pressure gradually increased from 5 MPa to 20 MPa. At 0 wet–dry cycles (Figure 4a), the peak strength of the sample with a confining pressure of 5 MPa was approximately 160 MPa; meanwhile, when the confining pressure increased to 20 MPa, the peak strength rose to approximately 190 MPa, an increase of nearly 19%. This phenomenon can be attributed to the suppressive effect of confining pressure on pore pressure and its effective constraint on microcrack propagation. Under high confining pressure, lateral stress helps to close existing microcracks, enhances interparticle bonding, and delays the propagation of macrocracks, thereby improving the overall stability of the material. Simultaneously, the increase in confining pressure alters the rock's failure mode, gradually transitioning from brittle fracture to ductile deformation, characterized by a smoother softening phase and higher residual strength. Furthermore, with increasing confining pressure, the nonlinear hardening stage before reaching its peak value becomes more pronounced. Therefore, confining pressure inhibits the initiation and propagation of microcracks within the limestone and enhances the normal contact stress between

particles, thus improving its load-bearing capacity. Typically, under zero-cycle conditions, the strength corresponding to a confining pressure of 20 MPa (approximately 200 MPa) is significantly higher than that under a confining pressure of 5 MPa (approximately 160 MPa).

As shown in Figure 7, the degradation rate of limestone showed a significant nonlinear increase with the number of wet–dry cycles, exhibiting a clear cumulative damage effect: at 5 cycles, the degradation rates under various confining pressures were 9%, 7%, 7%, and 0%, respectively; at 10 cycles, they were 13%, 13%, 22%, and 4%; at 15 cycles, they were 25%, 21%, 27%, and 21%; at 25 cycles, they were 38%, 25%, 31%, and 31%; and at 50 cycles, they reached 47%, 44%, 46%, and 38%, respectively. Confining pressure had a certain inhibitory effect on the degradation process, especially at higher cycle stages; for example, at 50 cycles, the degradation rate under 20 MPa was 9 percentage points lower than that under 5 MPa. The results indicate that limestone damage under wet–dry cycles has significant cumulative and accelerated evolution characteristics, while higher confining pressure can effectively inhibit fracture propagation and delay the degradation of mechanical properties.

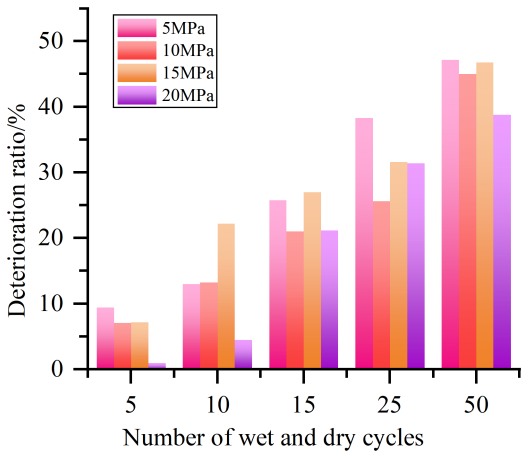


Figure 7. Columnar diagram of peak compressive strength degradation of limestone under different wet–dry cycles.

Figure 8 illustrates the variation in peak compressive strength of limestone with confining pressure under different wet–dry cycle conditions. This can be analyzed from two perspectives: Under all wet–dry cycle conditions, the peak compressive strength shows a monotonically increasing trend with increasing confining pressure, exhibiting a typical confining pressure strengthening effect. Taking 0 cycles as an example, the strength increases from approximately 160 MPa (5 MPa confining pressure) to approximately 200 MPa (20 MPa confining pressure), an increase of approximately 40 MPa; under 5 cycles, it increases from approximately 150 MPa to approximately 195 MPa, an increase of approximately 45 MPa; and under 10 cycles, it increases from approximately 140 MPa to approximately 190 MPa, an increase of approximately 50 MPa. Similar patterns are observed under other cycle numbers, such as increasing from approximately 85 MPa to approximately 120 MPa after 50 cycles. This indicates that increasing confining pressure effectively improves the bearing capacity of the rock mass, essentially due to the inhibitory effect of confining pressure on fracture closure and propagation. Simultaneously, it can be seen that as the number of wet–dry cycles increases, all curves shift downwards overall, indicating a continuous decrease in strength level.

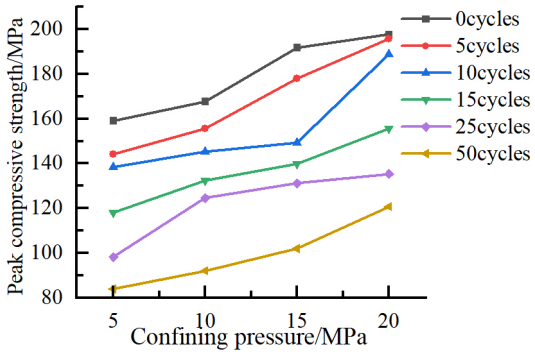


Figure 8. Peak compressive strength of limestone under different confining pressures.

From the perspective of the effects of wet–dry cycles, under the same confining pressure, the peak strength decreases significantly with increasing cycle count. For example, under a confining pressure of 20 MPa, the strength gradually decreases from approximately 200 MPa after 0 cycles to approximately 120 MPa after 50 cycles, a decrease of 80 MPa; under a confining pressure of 5 MPa, it decreases from approximately 160 MPa to approximately 85 MPa, a decrease of approximately 75 MPa. This indicates that wet–dry cycles have a significant weakening effect on rock mass strength, and this degradation effect accumulates with increasing cycle count. Combined with the degradation rate variation pattern shown in the previous figure, it can be seen that the degradation rate increases with increasing cycle count, while the strength decreases accordingly, showing a good correlation between the two. Furthermore, under high confining pressure, the degradation rate is lower while the strength remains higher, further indicating that confining pressure can, to some extent, delay the damage evolution caused by wet–dry cycles.

Combining the degradation rate variation with the number of wet–dry cycles shown in the previous figure, it can be seen that the two exhibit corresponding evolutionary characteristics: wet–dry cycles lead to a continuous increase in the degradation rate, while the compressive strength decreases overall. Simultaneously, the confining pressure has a consistent effect on both; that is, increasing the confining pressure reduces the degradation rate while increasing the compressive strength. Especially in the high-cycle stage, the strength attenuation is more significant under low confining pressure, while high confining pressure can, to some extent, offset the damage accumulation caused by wet–dry cycles.

Wet–dry cycles significantly affect the stress–strain curve characteristics of limestone by inducing internal material damage (such as the initiation, propagation, and penetration of microcracks). As the number of cycles increases from 0 to 50, the peak strength continuously decreases, while the peak strain shows a trend of first increasing and then decreasing or fluctuating, reflecting the gradual degradation of the material's mechanical properties by the cyclic action. In the early stages of cycling (0–15 cycles), the peak strength decreases rapidly, indicating that early wet–dry cycles can cause significant damage accumulation; as the number of cycles further increases to 25–50 cycles, the strength attenuation rate tends to slow down, indicating that the internal structure of the material gradually stabilizes under repeated cycling. Meanwhile, wet–dry cycling also leads to a decrease in the slope of the initial segment of the stress–strain curve (i.e., a decrease in the elastic modulus), an increase in the slope of the softening segment after the peak, and a continuous decline in residual strength, reflecting the deterioration in material stiffness and enhanced ductile failure characteristics.

From the perspective of peak strength evolution, the number of wet–dry cycles is the dominant factor controlling the degradation of the mechanical properties of limestone. With increasing cycle count, the strength decrease widens; for example, after 50 cycles, the peak strength of the sample is significantly lower than its initial state, indicating that long-term

cycling has a continuous weakening effect on structural integrity. This is mainly because the repeated immersion–drying process promotes the expansion and connectivity of pore structures, exacerbates mineral dissolution and interface weakening, and gradually transforms the internal structure from dense to loose. Furthermore, with increasing cycle count, the strength differences under different working conditions gradually decrease, indicating that continuous damage accumulation makes the material's mechanical response more uniform, further demonstrating the dominant effect of wet–dry cycling on the mechanical properties of the rock mass.

4.2. The Deteriorating Effect of Wet–Dry Cycling on the Mechanical Properties of Limestone

The mechanical properties of rocks can reflect their macroscopic mechanical behavior from different perspectives. The elastic modulus characterizes the deformation capacity and stiffness of rock masses under stress, and is an important indicator of a material's resistance to elastic deformation. Cohesion reflects the degree of cementation within the rock mass and the strength of interparticle bonding, demonstrating the structural contribution to its shear strength. The internal friction angle characterizes the friction and interlocking ability between particles and is an important parameter controlling the shear strength of rock masses. Poisson's ratio reflects the response characteristics of a material to lateral deformation under axial compression. These parameters collectively determine the deformation and failure behavior of rock masses during loading.

To systematically analyze the evolution of the mechanical properties of limestone under different wet–dry cycles, various mechanical parameters were extracted based on the stress–strain curve data shown in Figure 4. Considering that the differences in mechanical parameters under different confining pressures are relatively small under the same wet–dry cycle conditions, the average value of the parameters obtained under each confining pressure condition was taken to characterize the overall mechanical properties under that number of cycles. The calculated mechanical parameters of limestone under different wet–dry cycles are shown in Table 1, and curves showing the relationship between each mechanical parameter and the number of wet–dry cycles were plotted accordingly.

Table 1. Mechanical properties of limestone under different dry–wet cycling conditions.

Number of Wet–Dry Cycles	Modulus of Elasticity/GPa	Poisson's Ratio	Cohesion/MPa	Internal Friction Angle/°
0	22.98	0.23	146.01	58.99
5	21.24	0.22	125.10	54.05
10	20.42	0.22	116.71	52.04
15	19.22	0.21	106.54	47.76
25	16.30	0.20	94.98	47.05
50	14.49	0.19	78.90	46.85

As shown in Figure 9, both the elastic modulus and Poisson's ratio of the limestone exhibit a significant decreasing trend with increasing wet–dry cycle count, and the overall change is nonlinear. The elastic modulus gradually decreases from approximately 23 GPa at 0 cycles to approximately 14.5 GPa at 50 cycles, a decrease of approximately 37.0%, indicating that wet–dry cycles significantly weaken the rock mass stiffness. In the 0–15 cycle stage, the elastic modulus decreases rapidly, from approximately 23 GPa to approximately 19 GPa, a decrease of approximately 17.4%. However, in the 15–50 cycle stage, the rate of decrease slows significantly, indicating that the initial cycles cause more severe damage to the rock mass structure, while the damage gradually stabilizes in the later stages. Poisson's ratio shows a similar pattern, gradually decreasing from approximately 0.226 to approximately 0.197, an overall decrease of approximately 12.8%. The decrease is most

pronounced in the 0–10 cycle stage, followed by a slower rate of change, reflecting that wet–dry cycles cause the internal structure of the rock mass to gradually shift from dense to loose, and the lateral deformation capacity gradually weakens. A similar phenomenon has also been reported in previous studies. For example, Shao et al. investigated the mechanical behavior of deep tight sandstone under dry–wet alternations and found that both the dynamic Young's modulus and Poisson's ratio decreased after repeated dry–wet cycles [35]. In addition, Yang et al. reported that dry–wet cycling caused a continuous decrease in rock strength, elastic modulus, and acoustic velocity, which was closely related to changes in particle characteristics and pore distribution after water–rock interaction [36]. These findings support the decreasing trend of Poisson's ratio observed in this study and indicate that the reduction in Poisson's ratio is a reasonable mechanical response associated with wet–dry-cycle-induced internal damage.

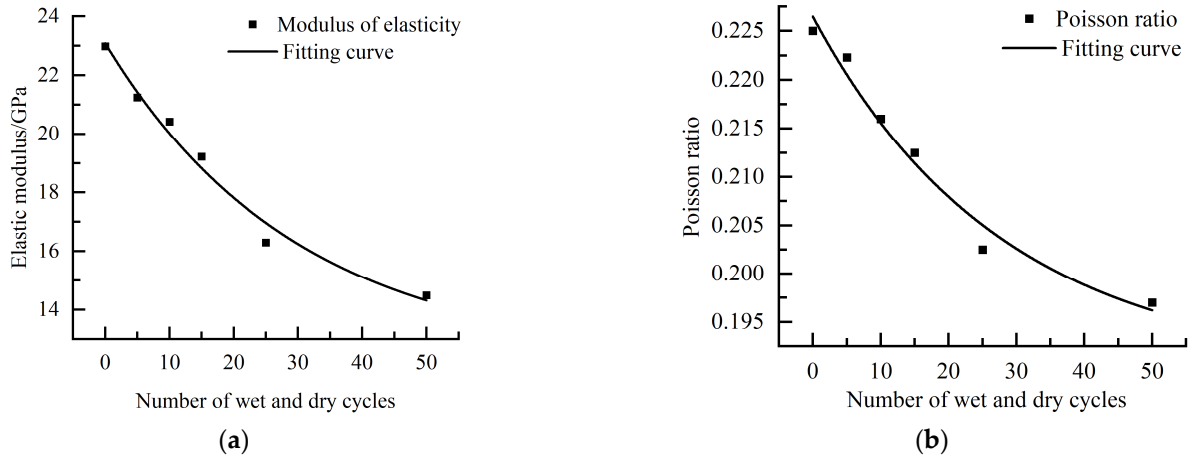


Figure 9. Deterioration curves of elastic modulus and Poisson's ratio of limestone under wet–dry cycles. (**a**) Relationship between elastic modulus and number of wet–dry cycles. (**b**) Relationship between Poisson's ratio and number of wet–dry cycles.

From a mechanistic perspective, the repeated expansion and contraction due to water absorption during the wet–dry cycle promotes the initiation and expansion of microcracks within the rock mass, and exacerbates the weakening of interfaces and cementation failure between mineral particles, leading to a gradual deterioration of the load-bearing framework and a continuous decrease in the elastic modulus. Simultaneously, the expansion and connection of cracks weakens the material's lateral deformation coordination ability under compression, causing a downward trend in Poisson's ratio. This is because the development of microcracks and the weakening of interparticle bonding reduce the integrity of the rock skeleton, thereby limiting the coordinated lateral deformation response under axial compression. Therefore, the decrease in Poisson's ratio can be interpreted as the result of accumulated microstructural damage and deterioration of deformation compatibility caused by repeated wetting and drying. Furthermore, function fitting of the experimental data shows that both the elastic modulus and Poisson's ratio can be well described by exponential decay functions, with correlation coefficients of 0.9782, 0.9684, 0.9943, and 0.9869, indicating a high degree of consistency between the fitting results and the experimental data. In summary, the impact of the wet–dry cycle on the mechanical parameters of limestone exhibits a significant stage-specific characteristic: "rapid deterioration in the initial stage–gradual stabilization in the middle and later stages." This pattern is of great significance for assessing the long-term evolution of the mechanical properties of the rock mass on reservoir slopes.

To further reveal the essence of the degradation of the mechanical properties of limestone under wet–dry cycles, a damage variable D can be introduced based on the attenuation of macroscopic mechanical parameters. Considering that the elastic modulus can effectively characterize the internal structural integrity of the material, the damage variable based on the elastic modulus is defined as:

$$D = 1 - \frac{E_N}{E_0} \tag{1}$$

In the formula, E_0 is the elastic modulus in the initial state (N = 0), and E_N is the elastic modulus after the Nth wet–dry cycle.

Substituting Equation (1) into the above definition, the evolution relationship of the damage variable with the number of wet–dry cycles can be obtained as follows:

$$D = 1 - \frac{11.25 \times 0.97^N + 12.01}{E_0} \tag{2}$$

where $E_0 = 11.25 + 12.01 = 23.26$ GPa. Further simplification yields:

Therefore, the damage variable D increases monotonically with the number of wet–dry cycles, and the rate of increase gradually slows down, exhibiting obvious exponential evolution characteristics. This reflects the process of damage within the rock mass gradually developing from rapid accumulation to stability.

Based on this, by introducing the classical continuous damage mechanics assumption, an equivalent constitutive relation considering the effects of wet–dry cycles can be established:

$$\sigma = (1 - D)\, E_0\, \varepsilon \tag{3}$$

In the formula, σ represents stress, ε represents strain, and $(1 - D)E_0$ represents the equivalent elastic modulus after damage. This model can describe the influence of rock mass stiffness degradation on the overall mechanical response under wet–dry cycle conditions.

As shown in Figure 10, both the cohesion and internal friction angle of the limestone exhibit a significant decreasing trend with increasing wet–dry cycle frequency, but their variation characteristics differ somewhat. The cohesion gradually decreased from an initial 146.01 MPa to 78.90 MPa, a total decrease of 46.0%, indicating that wet–dry cycles significantly weaken the structural strength of the rock mass. During the change, the cohesion showed a continuous monotonically decreasing trend, with a faster decrease in the early stage (0–15 cycles) followed by a gradual slowdown, demonstrating typical exponential decay characteristics. In contrast, the internal friction angle decreased from 58.99° to 46.85°, a decrease of approximately 20.6%, with a smaller overall change than that of the cohesion. This suggests that the impact of wet–dry cycles on interparticle friction and interlocking is relatively limited, and the decrease in shear strength is mainly controlled by the cohesion.

Fitting analysis of the experimental data shows that the cohesion and internal friction angle satisfy exponential decay relationships:

$$c = 74.25 \times 0.95^N + 74.26 \tag{4}$$

$$\phi = 13.06 \times 0.90^N + 46.26 \tag{5}$$

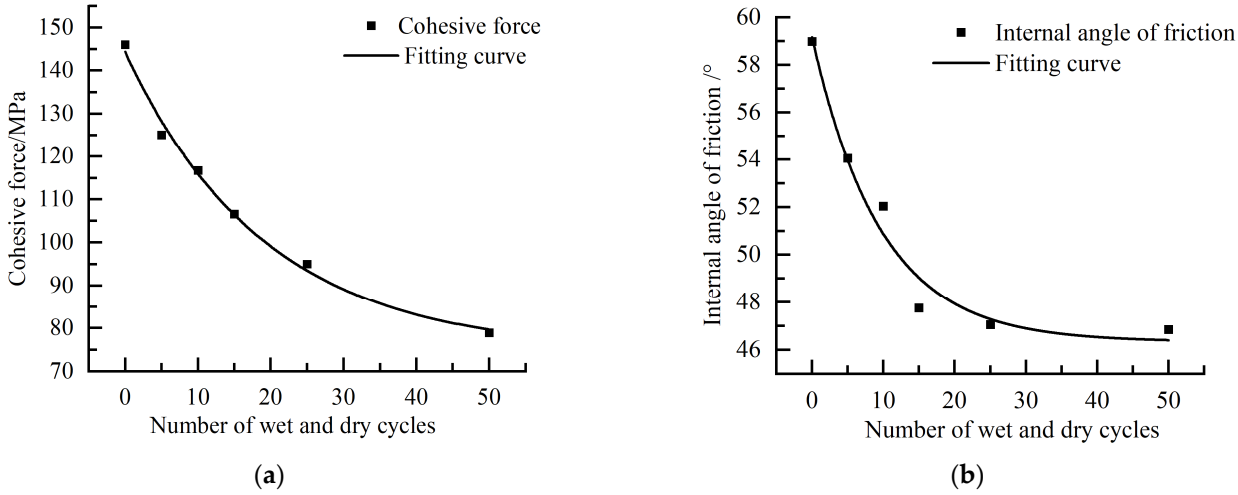


Figure 10. Deterioration curves of limestone cohesion and internal friction angle under wet–dry cycles. (**a**) Relationship between cohesion and number of wet–dry cycles. (**b**) Relationship between internal friction angle and number of wet–dry cycles.

The correlation coefficients were 0.9782, 0.9684, 0.9943, and 0.9869, respectively, indicating a good fit.

Equation (4) shows that the cohesion gradually approaches a stable value of 74.26 MPa with increasing wet–dry cycle count, indicating that under long-term cyclic action, the structural cementation strength of the rock mass tends to the residual level; the attenuation coefficient of 0.95 reflects that its deterioration process is relatively slow but continuous. Equation (5) shows that the internal friction angle tends to a stable value of 46.26° with increasing cycle count, and the attenuation coefficient of 0.90 indicates that its initial decrease is relatively faster, but the overall change is limited. In summary, the deterioration of the shear strength parameters of limestone under wet–dry cycle action is mainly due to the attenuation of cohesion, while the change in internal friction angle is relatively minor. This is consistent with the cementation failure and microcrack development mechanism caused by wet–dry cycle action. From the perspective of strength criteria, based on the Mohr–Coulomb criterion, with the increase in the number of wet–dry cycles (N), the synchronous decay of cohesion (C) and internal friction angle (φ) will cause the overall strength envelope to shift downward and slightly slow down, manifested as a decrease in intercept and slope, thus reflecting the continuous reduction in the shear strength of the rock mass and the gradual degradation of the failure envelope.

Analysis of the triaxial compression test data and failure characteristics of limestone reveals that after undergoing wet–dry cycles, the mechanical properties of limestone, including compressive strength, elastic modulus, Poisson's ratio, cohesion, and internal friction angle, exhibit similar and significant deterioration. This deterioration is not merely a numerical change but is directly reflected in the load-bearing capacity of the limestone. The decrease in compressive strength directly indicates a weakening of the limestone's ability to withstand pressure, leading to a reduced load-bearing capacity and increased susceptibility to failure under external loads; the decrease in elastic modulus signifies a weakening of the limestone's deformation capacity under stress. When subjected to external forces, limestone's resistance to deformation decreases, making it more prone to deformation. Changes in Poisson's ratio reflect an alteration in the ratio of lateral to longitudinal deformation during stress, affecting not only the deformation characteristics of the limestone but also its overall stability. Cohesion, the force attracting particles within the rock, weakens the internal binding force, making the limestone more susceptible to disintegration under external forces. Conversely, a decrease in the internal friction angle,

the force of friction between particles, directly leads to increased susceptibility to sliding failure under shear forces.

Therefore, alternating wet and dry cycles have a significant impact on the deterioration of limestone. This deterioration not only weakens the overall mechanical properties of the rock but also increases the instability of the slope rock mass under external loads.

5. Conclusions

The main conclusions are as follows:

The peak strength of limestone increases with confining pressure under all wet–dry cycle conditions, indicating a significant confining pressure strengthening effect.

The mechanical parameters of limestone exhibit progressive deterioration with increasing wet–dry cycles. After 50 cycles, the elastic modulus, cohesion, and internal friction angle decreased by 35.94%, 45.98%, and 21.13%, respectively. The deterioration process follows an exponential trend characterized by rapid initial degradation and gradual stabilization.

Wet–dry cycling significantly alters the failure characteristics of limestone, promoting the transition from single-crack propagation to multi-crack coalescence and fragmentation, accompanied by enhanced brittleness. Higher confining pressure effectively suppresses crack propagation and reduces the deterioration amplitude.

Based on damage mechanics theory, a constitutive relationship considering the influence of wet–dry cycles was established to characterize the degradation of rock stiffness and its effect on the overall mechanical response under cyclic wetting–drying conditions.

This study reveals the degradation characteristics of limestone mechanical properties under coupled confining pressure and wet–dry cycles, providing experimental and theoretical support for the stability evaluation and engineering design of reservoir bank slopes.

Author Contributions: Z.Y.: Conceptualization, Data curation, Resources. S.Z.: Funding acquisition, Investigation. P.L.: Formal analysis, Methodology, Validation. R.A.: Project administration, Supervision. G.D.: Writing—original draft, Visualization. Z.Z.: Data curation, Formal analysis, and Writing—review and editing. All authors have read and agreed to the published version of the manuscript.

Funding: This research was funded by the Scientific Research Projects of China Three Gorges Corporation (Project No.: WDD/0578).

Data Availability Statement: The datasets generated during and/or analyzed during the current study are available from the corresponding author on reasonable request.

Acknowledgments: The authors sincerely thank the project leader, faculty, and students for their invaluable support. We are very grateful for their assistance throughout the data collection, research implementation, and engineering processes. We also thank the anonymous reviewers and editors for taking the time to review this paper and providing valuable feedback that greatly contributed to the progress of the research.

Conflicts of Interest: Authors Zongli Yang and Shaowu Zhou are employed by China Three Gorges Construction (Group) Co., Ltd. The remaining authors declare that the research was conducted in the absence of any commercial or financial relationships that could be construed as a potential conflict of interest. Authors Peng Lin and Ruinan An are employed by Tsinghua University. The remaining authors declare that the research was conducted in the absence of any commercial or financial relationships that could be construed as a potential conflict of interest. Authors Guoyong Duan and Zhongyan Zhao are employed by China Three Gorges University. The remaining authors declare that the research was conducted in the absence of any commercial or financial relationships that could be construed as a potential conflict of interest.

References

1. Zhang, X.; Luo, Y.; Song, K.; Gong, H.; Zhang, M.; Li, X. Impact resistance and degradation model of reinforced reef limestone concrete composite under wet-dry carbonation cycles. *Structures* **2010**, *79*, 18.
2. He, Z.M.; Liu, X.Q.; Huang, K.; Xiong, J.P. Seepage and Dynamic Characteristics of Carbonaceous Mudstone Coarse-Grained Soil Embankment with Different Gradations. *Adv. Civ. Eng.* **2025**, *2021*, 4436942.
3. Wang, C.; Zhang, Q.; He, M.; Guo, S.; Jia, Y. Mechanism of Fracture Process Zone Development in Sandstone and Limestone Under Mode I Loading Wet–Dry Cycles and Temperature. *Rock Mech. Rock Eng.* **2025**, *58*, 7307–7328. [CrossRef]
4. Chen, Y.; Xie, Q.; Zhang, H.; Tu, Z.; Lei, X.; Fu, X. Mechanism of limestone degradation under alkaline wet-dry cycles using mel-frequency cepstral coefficient. *Eng. Geol.* **2010**, *357*, 19.
5. Zhou, Z.; Cai, X.; Chen, L.; Cao, W.; Zhao, Y.; Xiong, C. Influence of cyclic wetting and drying on physical and dynamic compressive properties of sandstone. *Eng. Geol.* **2017**, *220*, 1–12. [CrossRef]
6. Ge, Q.; Wu, H.; Gong, Y.F. Research on the Soil Slope Stability Based on Soil Strength Deterioration in Seasonal Frozen Areas. *Adv. Mater. Res.* **2011**, *243*, 4270–4273. [CrossRef]
7. Beck, K.; Al-Mukhtar, M. Cyclic wetting–drying ageing test and patina formation on tuffeau limestone. *Environ. Earth Sci.* **2014**, *71*, 2361–2372.
8. Hale, P.A.; Shakoor, A. A Laboratory Investigation of the Effects of Cyclic Heating and Cooling, Wetting and Drying, and Freezing and Thawing on the Compressive Strength of Selected Sandstones. *Environ. Eng. Geosci.* **2003**, *9*, 117–130. [CrossRef]
9. Lin, M.L.; Jeng, F.S.; Tsai, L.S.; Huang, T.H. Wetting weakening of tertiary sandstones—microscopic mechanism. *Environ. Geol.* **2005**, *48*, 265–275. [CrossRef]
10. Yang, Z.; Liu, M.; Zhang, S.; Gao, Y.; Hou, S. Damage evolution and constitutive model of limestone considering fissure angle and wet-dry cycles under axial stress. *Theor. Appl. Fract. Mech.* **2010**, *140*, 28.
11. Zhang, Y.; Wang, Z.; Su, G.; Wu, Z.; Liu, F. Experimental Investigation on Influence of Acidic Dry-Wet Cycles on Karst Limestone Deterioration and Damage. *Geofluids* **2022**, *2022*, 8562226. [CrossRef]
12. Wang, G.L.; Zhang, T.; Zhang, L. The law of strength damage and deterioration of jointed sandstone after dry-wet cycles. *J. Mt. Sci.* **2023**, *20*, 1170–1182. [CrossRef]
13. Huang, K.; Cai, G.; Zha, F.; Kang, B.; Wang, Q.; Shen, Y. Damage Mechanism Evolution of Argillaceous Siltstone Exposed to Dry–Wet Cycles: Experimental, Theoretical and Numerical Study. *Rock Mech. Rock Eng.* **2026**, *59*, 43–64.
14. Li, T.; Yang, Z.; Ma, D.; Tian, J.; Feng, H. Effects of dry–wet cycles on the dynamic characteristics of cement-stabilized loess. *Bull. Eng. Geol. Environ.* **2025**, *84*, 433. [CrossRef]
15. Yuan, G.; Cao, Y.; Xi, K.; Wang, Y.; Li, X.; Yang, T. Feldspar dissolution and its impact on physical properties of Paleogene clastic reservoirs in the northern slope zone of the Dongying sag. *Acta Pet. Sin.* **2013**, *34*, 853–866. [CrossRef]
16. Li, X.; Yan, B.; Wang, Q.; Hong, Z.; Zhang, Y.; He, C. Wave Velocity Evolution Law and Mechanical Index Attenuation Model of Limestone under Different Freeze-thaw Cycles. *Results Eng.* **2025**, *26*, 105216. [CrossRef]
17. Huang, C.; Zhu, C.; Ma, Y. Investigating Mechanical Characteristics of Rocks Under Freeze–Thaw Cycles Using Grain-Based Model. *Rock Mech. Rock Eng.* **2025**, *58*, 603–622. [CrossRef]
18. Liu, X.; Li, Y.; Wang, W. Study on mechanical properties and energy characteristics of carbonaceous shale with different fissure angles under dry–wet cycles. *Bull. Eng. Geol. Environ.* **2022**, *81*, 319. [CrossRef]
19. Tian, Y.; Yu, R.G. Energy analysis of limestone during triaxial compression under different confining pressures. *Yantu Lixue/Rock Soil Mech.* **2014**, *35*, 118–122, 129.
20. Ijaz, N.; Ye, W.; Wang, Q.; Chen, Y.; ur Rehman, Z.; Ijaz, Z.; Khalid, U. A hydraulic binder for compacted clay under wet-dry cycles: Low carbon limestone calcined clay cement. *Chin. J. Rock Mech. Geotech. Eng.* **2025**, *17*, 5970–5988. [CrossRef]
21. Sheshde, E.A.; Cheshomi, A.; Maleki, R. Estimation of shear strength parameters of intact limestones using miniature triaxial test. *Eng. Geol.* **2024**, *334*, 107509. [CrossRef]
22. Gao, P.; He, J.; Ding, J. Large-Scale Triaxial Tests on Dissolved-Weathered Limestone Rockfill Considering Particle Breakage. *Geotech. Geol. Eng.* **2026**, *44*, 47. [CrossRef]
23. Wang, Z.; Zeng, Z.; Lyu, C.; Wang, M.; Hu, X.; Dong, Y. Time-dependent behavior and permeability evolution of limestone under hydro-mechanical coupling. *J. Mt. Sci.* **2024**, *21*, 1697–1714. [CrossRef]
24. Peng, Q.; Li, K.; Shi, J.; Li, M.; Qin, Q. Study on the triaxial creep and acoustic emission characteristics of surrounding rock in high-stress caverns under different initial damage levels. *Front. Earth Sci.* **2025**, *13*, 1598270. [CrossRef]
25. Wu, W.; Zhao, L.; Lai, Y.; Lv, Z.; Chen, Y.; Ran, J. A rational multiscale nonlinear constitutive model for freeze–thaw rocks under triaxial compression. *Int. J. Plast.* **2024**, *179*, 104040. [CrossRef]
26. Li, C.; Wang, C.; Zuo, Y.; Li, Z.; Yong, C.; Wu, M. Damage Evolution Modeling of Karst-Affected Dolomite Under Uniaxial Compression. *Geotech. Geol. Eng.* **2025**, *43*, 328. [CrossRef]
27. Dai, W.; Gao, P.; Cheng, B.; Pan, C. Experimental study on the dynamic tensile behavior and energy evolution of limestone subjected to dry-wet cycles. *Front. Mater.* **2025**, *12*, 1571855. [CrossRef]

28. Tan, D.; Cheng, H.; Hou, C.; Lei, Y.; Jiang, C.; Zhao, Y.; Zhang, H. Experimental Study on the Effects of Dynamic High Water Pressure on the Deformation Characteristics of Limestone. *Appl. Sci.* **2025**, *15*, 42. [CrossRef]
29. Dong, W.; Li, Z.; Shen, L.; Liu, W.; Guo, Y.; Xu, H.; Yong, R. Study on the process of mass transfer and deterioration of limestone under dynamic dissolution of CO_2 solution. *Sci. Rep.* **2024**, *14*, 5278. [CrossRef] [PubMed]
30. Wang, Z.J.; Liu, X.-R.; Fu, Y.; Zhang, L.; Yuan, W. Deterioration of mechanical parameters of argillaceous sandstone under wetting-drying cycles in acidic environment. *Chin. J. Geotech. Eng.* **2016**, *38*, 1152–1159.
31. Zhang, F.; Yin, W.; Xian, L.; Liu, M.; Yuan, Z.; Jiang, H. Triaxial creep characteristics and microstructure of red sandstone under acidic dry-wet cycles. *Phys. Scr.* **2025**, *100*, 095014. [CrossRef]
32. Leng, F.; Rong, J.; Ding, W.; Tian, G.; Zhou, Y.; Ji, X.; He, G.; Wei, Q.; Wang, J.; Bao, K. Introduction to GB/T50082-2009 "Standard for Test Methods of Long-Term Performance and Durability of Ordinary Concrete". *Constr. Technol.* **2010**, *39*, 6–9.
33. Deng, T. Study on shear strength characteristics and estimation model of limestone under different weathering degrees. *Hydrogeol. Eng. Geol.* **2022**, *49*, 10.
34. Ding, W. Study on mechanical and chemical dissolution characteristics of limestone under chemical solution erosion. *Rock Soil Mech.* **2015**, *36*, 6.
35. Shao, J.; Kang, Y.; You, L.; Chen, M. Effect of dry-wet alternations on the mechanical strength of deep tight sandstone. *J. Pet. Sci. Eng.* **2021**, *204*, 108750. [CrossRef]
36. Yang, X.; Wang, J.; Hou, D.; He, M. Effect of Dry-Wet Cycling on the Mechanical Properties of Rocks: A Laboratory-Scale Experimental Study. *Processes* **2018**, *6*, 199. [CrossRef]

Disclaimer/Publisher's Note: The statements, opinions and data contained in all publications are solely those of the individual author(s) and contributor(s) and not of MDPI and/or the editor(s). MDPI and/or the editor(s) disclaim responsibility for any injury to people or property resulting from any ideas, methods, instructions or products referred to in the content.